Changing the approach to sustainable constructions: An adaptive mix-design calibration process for earth composite materials

M. Franciosi[1], V. Savino [1] , L. Lanzoni [2], A. M. Tarantino [2], M. Viviani [1]

[1] Département d'Environnement Construit & Géoinformation, University HES-SO / HEIG-VD, CH-1401 Yverdon-les-Bains, Switzerland

[2] Department of Engineering "Enzo Ferrari", University of Modena and Reggio Emilia, 41125 Modena, Italy

Abstract

One major drawback of excavation earth-based composite construction materials is the variability in excavation earth characteristics from site to site. This variability can affect certain physical properties, and, in turn, the design models used to create a structure. To solve this problem, a methodology has been developed to predict the physical properties of earth-based composites for any mix-design variation, which enables a robust structural design process.

This new methodology has been tested for Shot-earth, a new class of earth-based composite material made using high rates of excavation earth, aggregates, and a low rate of stabilization if needed. Shot-earth is placed using a high-speed dry-mix process.

The methodology was tested by preparing small, inexpensive specimens through a process that simulates the dry-process used to fabricate Shot-earth in the field. An adaptive technique, used in conjunction with the experimental methodology, allows for the identification of the variant of possible Shot-earth mix-designs that provides optimal physical properties for a specific project. This technique is potentially applicable to any type of earth-based composite. The proposed methodology's reliability enables a fast and cost-effective detailing of Shot-earth constructions.

Keywords: Earthen materials, eco-building constructions, mechanical characterization, mix-design optimization, experimental campaign.

1. Introduction

For thousands of years, soil has been utilized as a reliable construction material. In fact, the fortified city of Catalhöyük in Turkey, which dates back to 6000 BCE, was constructed using soil [1, 2]. This versatile material has been used to build some of the world's most iconic structures, including the Great Wall of China and the Pyramid of the Sun in Mexico, as depicted in Figure 1.

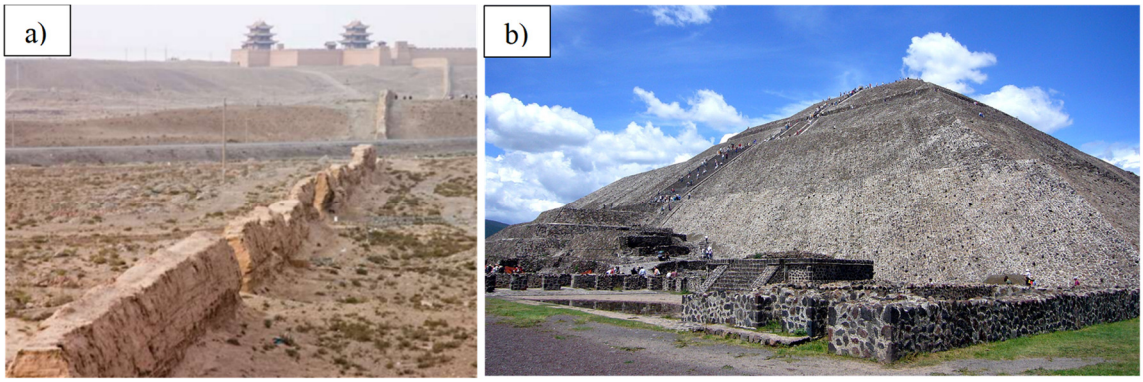

Figure 1. a) Great wall of China *[3]*, b) The pyramid of the Sun in Mexico [4].

The use and development of earthen construction techniques throughout the centuries have been strongly influenced by the availability of suitable earth and several socio-economic factors. Figure 2 displays a selection of sites where the rammed earth technique was used to construct buildings in different historical periods.

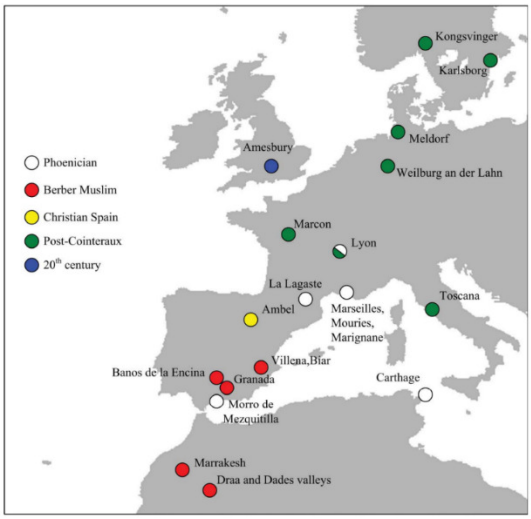

Figure 2: Chronological development of rammed earth techniques in Europe [5]**.**

Today, there are still three main types of traditional earthen construction techniques used for constructing single or two-story buildings: adobe, cob, and rammed earth [5, 6]. Adobe is primarily used to produce earthen blocks utilized to construct walls, vaults, arches, and domes, which are difficult or even impossible to construct with rammed earth [7, 8, 9, 10]. Earthen blocks are manufactured by compacting a mixture of wet soil and other compounds into a formwork [11]. Comprehensive studies on optimizing the compaction process to manufacture earth blocks are provided in [12, 13, 14]. Cob is a wet mixture of earth and vegetal fibers [6], piled or molded to create walls. Cob structures are built in layers, often referred to as lifts. Each lift has a height of 0.6-0.9 m and must be completely dried before the next layer can be added [8, 15]. Rammed earth is a technique where a mixture of moistened earth

and other compounds is compacted in superposed layers within a formwork [7]. Rammed earth is primarily used to construct walls, even in humid climates where building with adobe bricks is impractical or impossible [8]. Recent examples of rammed earth constructions are the Chapel of Reconciliation in Berlin and the Rauch House in Austria (see Figure 3).

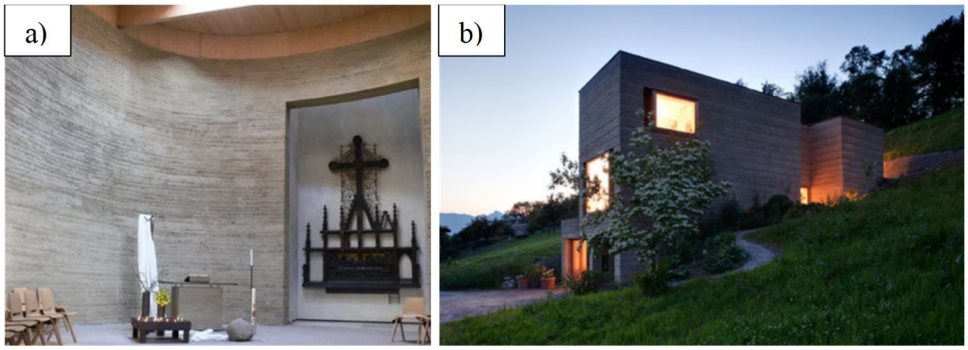

Figure 3: (a) Chapel of reconciliation in Berlin [16], (b) Rauch house in Austria [17].

Several studies focused on characterizing rammed earth from a mechanical standpoint can be found in the literature [18, 19, 20]. One of the most significant advantages of earthen constructions is their low cost and high sustainability due to the use of locally excavated and reusable raw materials, which require minimal processing energy, have a low carbon footprint, and reduce transportation-related ecological impacts [21, 22]. However, traditional earthen constructions have some major drawbacks, such as water sensitivity, low mechanical performance, high maintenance requirements, and labor intensiveness. Research has shown that the mechanical performance of soil-based materials can be enhanced by stabilizing them with binders such as Portland cement and lime [23]. Increasing the compaction energy is another method of improving the strength of earthen materials [24]. Recently, a novel excavation-based construction material called "Shot-earth" (hereafter labeled "SE") has been introduced as an alternative earth-based solution that overcomes the typical drawbacks of traditional earthen materials such as water sensitivity and low mechanical strength [25, 26]. SE is an ecological composite material that consists of a high percentage of soil excavated from a construction site, locally sourced coarse sand (0-16mm in size), and a small amount of stabilizer if required. The stabilizer can be hydraulic or hydrated lime, plaster, cement, or geopolymer. All ingredients are briefly homogenized in a special mixer before being projected at high speed (up to 300 km/h). The high-speed projection results in SE having high density (about 2100 kg/m3), excellent green strength, and lower water sensitivity. The composition of SE varies based on the designer's requirements and the type of excavation soil available at the construction site. Some soil types provide high strength without the need for stabilizer. High compaction of the mix increases the strength but also raises the thermal conductivity [27]. However, this is not a problem since the compaction level of SE can be reduced or a special mix of SE can be used for structural elements that require low thermal conductivity. Alternatively, the thermal transmittance

can be reduced by rendering the structural element with SE having low thermal conductivity [28, 29, 30, 31]. Rendering can also be done without waiting for the structural stabilized earth (SE) to dry. A particular care has always been paid to the predictability and repeatability of the mechanical performances of SE [25] [26]. The mix-design of SE must be adjusted for each new construction site, as the excavated soil varies from site to site, and its mechanical properties might change. A representative number of SE specimens should therefore be fabricated in each site, cured, and tested to develop reliable design models for the structural engineers. Several trials might be needed to adjust the mix and find the optimal recipe. This procedure is costly and time-consuming due to 1) the costs of manpower, equipment installation, excavation of a sufficient quantity of soil, and fabrication of SE specimens by projection at high speed, and 2) the costs required to deliver SE specimens to the nearest laboratory for conditioning and mechanical testing. A faster and low-cost approach to develop an SE – or another earth-based composite material- mix adapted to the engineers' needs is thus of great practical and economical interest. This paper presents a constitutive relationship able to predict the mechanical performance of SE by testing a small batch of pressed earth specimens (labeled hereafter as "PE"), whose fabrication is quicker and cheaper. In fact, PE specimens can be manufactured by compacting the SE mix that is under study in a mold. The present paper is organized into the following sections. In section 2, the materials and methods used in this work are described. In particular, this section presents an adaptive mix-design calibration process that can predict which PE mix-design will match the engineering properties of SE. The experimental analysis carried out on 28 trial PE mixtures of different mix-designs is also described. Section 3 includes an exhaustive discussion about the experimental results and presents a constitutive relationship between the engineering properties of SE and PE. Section 4 summarizes the main conclusions.

2. Materials and methods

2.1 Adaptive mix-design calibration process: control, input, output

In order to find an adapted PE mix-design that provides the same mechanical properties of SE an adaptive mix-design calibration process (labeled hereafter AMDCP) was used. A schematic illustration of its structure is reported in Figure 4.

2.1.1 AMDCP step 1

As shown in Figure 4, input parameters were selected to prepare trial PE mixture for mix-design analyses. According to the Literature [24, 32, 33, 34] mechanical properties of earth-based materials depend on several factors related to their mix-design, in particular water content (labeled hereafter "%w"), type (labeled hereafter "b") and amount of binder (labeled hereafter "%b"), use of grinded or not grinded earth (labeled hereafter "GE"), bulk density (labeled hereafter "BD") and compaction

pressure (labeled hereafter "p"). Consequently, all features abovementioned were considered in this investigation.

2.1.2 AMDCP steps 2 and 3

By fixing input parameters, a trial PE mixture was fabricated, cured and tested (*step 2*), see sections 2.2, 2.3, 2.4 and 2.5 for more details. Experimental results obtained by testing the trial PE mixture were analyzed and organized as output values, see section 3 for more details.

2.1.3 AMDCP step 4

A control criterion is requested to find the adapted mix-design of the PE mixture which best fits the mechanical performances of SE presented in [25]. In order to accept or discharge the mix-design of a trial PE mixture analyzed in AMDCP input and output values of PE series were compared with the engineering properties of SE. The engineering properties of SE requested to complete a design model were considered as reference for the control criterion, in particular BD, 28-day compressive strength (labeled hereafter "C-28"), elastic modulus (labeled hereafter "EM") and Poisson's ratio (labeled hereafter "PR") [25]. Several features related to the compounds of SE were considered as well, i.e. %w, b and %b. The authors assumed a threshold value of the maximum scatter between each engineering property of SE and the corresponding one of the trial PE mixture on the basis of the scatter range of both mechanical property observed for SE in [25] and the trial PE mixture (labeled hereafter "σ_{PE}"), see Table 4. For sake of clarity we describe an example of the control step designed for a particular engineering property of SE, the EM: the scatter of EM measured on SE specimens in [25] was 10%, so the threshold value of scatter between $EM_{,SE}$ and $EM_{,PE} \pm \sigma_{PE}$ used in step 4 was assumed to be 10%, which corresponds to 971 MPa, see details in blue box in Figure 4. If discrepancy between $EM_{,SE}$ and $EM_{,PE} \pm \sigma_{PE}$ is superior to the threshold value (971 MPa) the trial PE mixture is discharged and a new PE mixture with different mix-design is manufactured. Then, all steps previously presented start again for a new trial PE mixture, as can be seen in Figure 4. The same control condition described before was used for all 7 engineering properties implemented in AMDCP, i.e. %w, b, %b, BD, C-28, EM and PR. The AMDCP stops when all control conditions are satisfied.

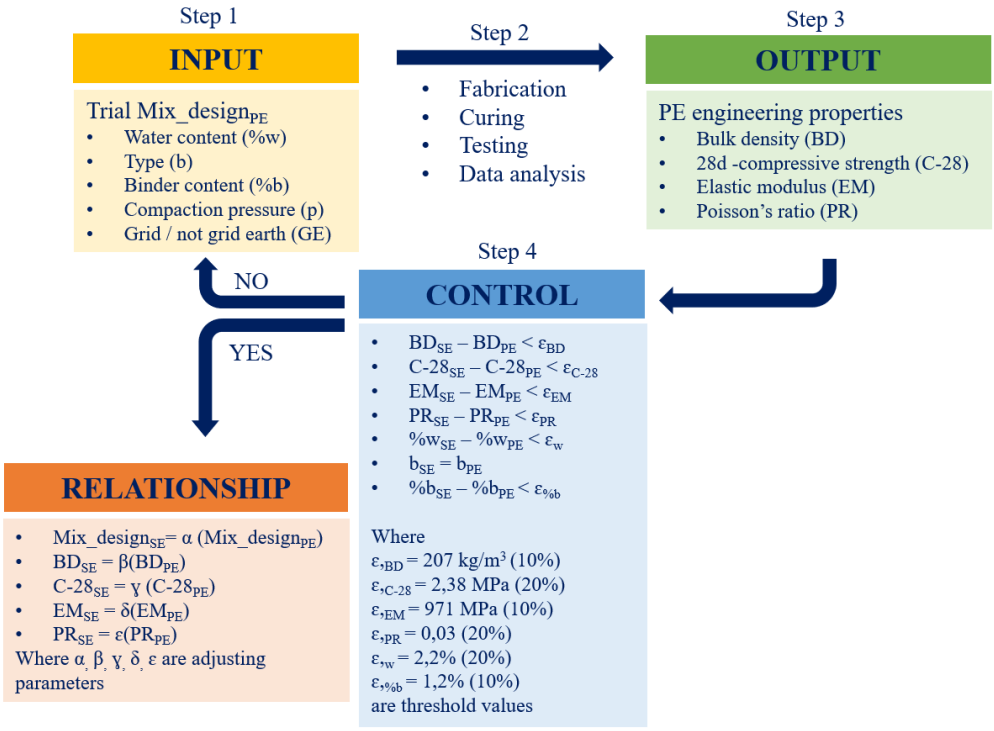

Figure 4. Flowchart of AMDCP.

Table 1. Water content in SE, excavated soil and coarse sand measured according to the standard protocol *[35]*

Specimen	Weight of wet specimen (g)	Weight of dry specimen (g)	Water content (%)
SE	24179.00	22460.40	8.67
Excavated soil	9796.90	8920.30	14.22
Coarse sand	13431.50	13183.30	2.38

Table 2. Engineering properties of SE used into the control criterion (step 4 of AMDCP) [25] .

Type of engineering properties	Average magnitude
Bulk weight	2067.3 kg/m^3
28 days compressive strength	9.50 MPa
Elastic modulus	9707 MPa
Poisson's ratio	0.15
Water content	8.66 %
Type of binder	CPC-42.5N
Binder content	12 %

2.2 design of the PE mixture

The soil used for fabricating all trial PE mixtures is the same used in SE presented in [25] as well as the amount of both excavated soil and coarse sand. For the sake of clarity, SE mix-design presented in the previous work was obtained by using 0.5 volume of excavated soil, 0.5 volume of coarse sand and 12% of cement by weight of the dry mixture. Further details about the features of the excavated soil and coarse sand used in this experimental program are reported in [26]. During the projection of SE 3% by volume of water was injected into the nozzle to promote cohesion and hydration of the cement present in SE. Though the amount of water added to the dry mix was known, the humidity of both coarse sand and excavated soil was not, especially for excavated soil whose humidity may change according to the climate conditions, e.g. it is higher in rainy seasons and lower in drought ones. According to the standard procedure reported in [35] Table 1 resumes the water content measured by authors in coarse sand and excavated soil used to fabricate SE in [25]. The water content of SE prior to the projection was measured as well. In Table 1 the water content (%w) is computed as drawn in Equation 1:

$$\%w = \left(\frac{w_w - w_s}{w_s}\right) \cdot 100\ (\%) \quad (1)$$

where w_w and w_s stand for weight for wet and dry SE specimens, respectively.

In order to fabricate PE, a rotational concrete panel mixer was used to mix raw materials together, see Figures 5a, 5b. In order to add the correct amount of water within the mixture, for each series investigated all raw materials were first oven-dried to remove their origin moisture [35]. It should be noted that the water level input to make SE varies according to the effective moisture present in excavated soils found at the construction site. In particular, excavated soils are wetter in rainy seasons than in drought ones. SE producers have defined a qualitatively and practical protocol to adjust the water content within the overall mixture, regardless of the humidity level of each raw material. This approach is inspired to the drop test described in African standard for rammed earth [36]. The same qualitatively protocol was used by authors to prepare trial PE mixtures in laboratory. After the consistence examination, the fresh PE mixture was poured in steel formworks. The specimens were then compacted. As indicator of adequate compaction level, BD_{PE} (see 'output' in Figure 4) was measured and compared with BD_{SE} (see 'control' in Figure 4). If the scatter was too high the compacting pressure was adapted to the next cycle in AMDCP, see Figure 4. After compaction, the PE specimen was demolded and covered with plastic sheets until the testing day. Figure 5c shows the PE specimens after demolding. All PE specimens were visually inspected prior to be cured and prepared for mechanical testing. It was observed that all PE specimens present a homogenous texture, quite similar to the texture of SE, with the only difference that interfacial zone between PE layers is not observed in SE, see Figure 5c and [25]. Once cured, prior to be tested, the upper surface of the specimens was smoothed, compensating the irregularity due to the compaction step for the upper layer. PE series were manufactured under laboratory conditions (20 ± 2 °C, 55 ± 10% RH). Each series was composed by four specimens, so experimental results, presented in the next sections, represent statistic values. This number of specimens for each

series made it possible to prepare all specimens within an hour, as recommended by [32]. In order to find a mechanical relationship between SE and PE, by using the AMDCP presented in section 2.1, the engineering properties of cured PE specimens were measured, in particular all properties useful to develop the design model of any construction building material, like BD, C-28, EM and PR, plus properties of mix-design, like %w, b and %b. The test setup requested for measuring C-28, EM and PR is explained in the following subsections.

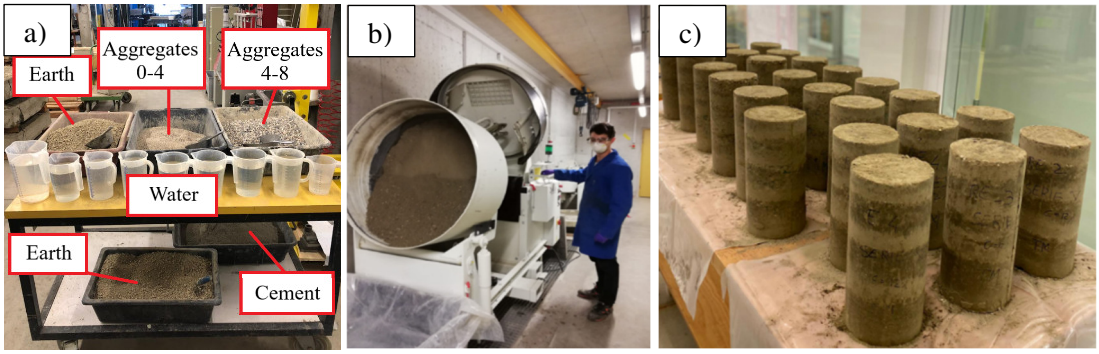

Figure 5. a) Raw materials used to make trial PE mixture, b) Rotation panel concrete mixer, c) PE specimens after demolding.

2.3 Compressive Test

The uniaxial compressive strength of PE was determined at 28 days ageing according to the European standard test adopted for concrete materials [37]. A 5000 kN force-controlled testing machine was used for compressive test, see Figure 6. The testing procedure was conducted in an unconfined configuration by applying a preloading of 15 kN and a loading rate of 0.3MPa/s, in agreement with standard. In some series a 7 days compressive strength was measured as well in order to speed up the AMDCP.

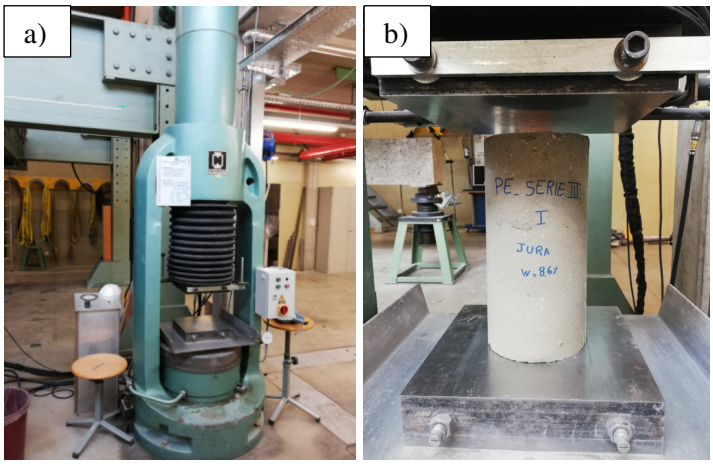

Figure 6. a) 5000 kN force controlled testing machine, b) Compression testing setup.

2.4 Elastic modulus test

The elastic modulus of PE was determined according to the European standard recognized for concrete material [38]. As for concrete specimen, a force-time diagram of three loading and unloading cycles was applied on PE specimens, see Figure 7. The first branch started from the preload and culminated at a force value corresponding to 30% of the C-28, with a loading rate of 0.3MPa/s. Then the loading remained constant for 20 seconds before going down. To complete the cycle the unloaded branch was characterized by the same rate as the loading one. Before taking the next cycle, the value of force is held constant for 20 seconds. The setup and disposition of gauge strain to measure the specimen deformation are showed in Figure 8a.

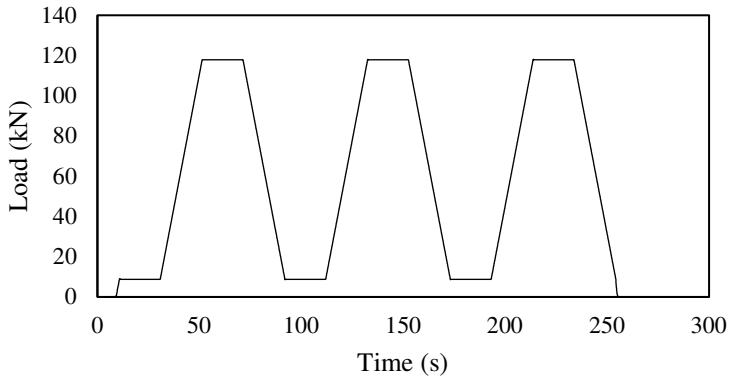

Figure 7. Force - Time diagram for EM test on PE specimens *[38]*

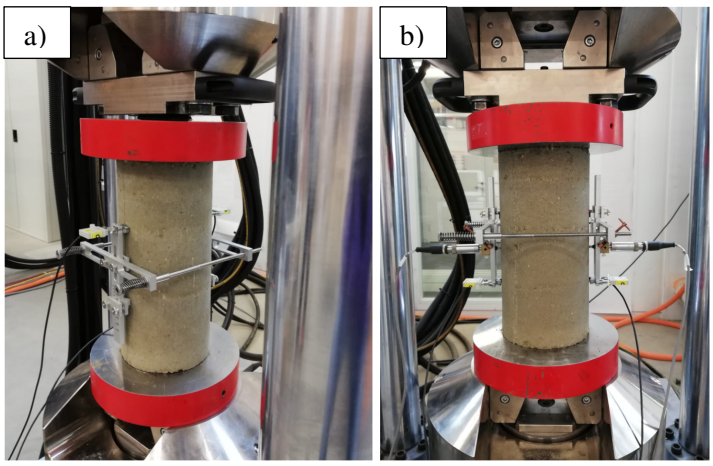

Figure 8. Experimental test to measure : a) EM, b) PR

2.5 Poisson ratio test

To evaluate the Poisson's ratio of PE the same force-time diagram used to estimate the elastic modulus was applied as well, according to the American standard [39]. However, the setup of gauge support was designed by the authors in order to be suitable for the specimen geometry. Compared to the EM setup previously presented, for PR test further strain gauges were placed orthogonally to the load line in opposite direction in order to evaluate the transverse strain too, see Figure 8b.

3. Results and discussion

The C-28, EM and PR tests were conducted for each trial PE mixtures designed by the AMDCP. The iterative process of AMDCP is stopped as soon as input and output value satisfy the control requirements, see Section 2.1 and Figure 4. Input and output data of the AMDCP are listed in Table 3, while the control check result is reported in Table 4. In control step the threshold values adopted for each mechanical parameter was defined by considering the expectable scatter of the engineering properties for earth/cement-based materials. The results showed in Table 3 indicate that the mechanical behavior of PE is strongly dependent on all input parameters here investigated, especially the %w, b and %b. On the basis of the experimental data %w must range from 6.5 to 9% to reach the optimum moisture content. Out of this range a drop of strength is observed, see series 1-11, 13 and 14 respectively. The use of GE does not seem to significantly influence the mechanical strength of PE, even though the requested power for mixing PE composed of GE can be reduced as fresh mixture was more workable. The important influence of the p magnitude highlighted by previous research [24] is confirmed by the experimental values in which the maximum strength is reached for p=10 MPa and minimum for almost p = 5.7 MPa.

Table 3. Input and output data implemented into the *AMDCP*

Series	INPUT					OUTPUT				
	w	b	%b	p	GE	BD	C-7	C-28	EM	PR
	%	-	-	MPa	-	kg/m^3	MPa	MPa	MPa	-
1	5.5	OPC-42.5N	6	9.05	no	2103.5 ± 11.6	4.31 ± 0.66	5.58 ± 1.07	4237 ± 224	-
2	5.78	OPC-42.5N	6	9.05	yes	2063.4 ± 9.7	-	5.92 ± 0.24	4718 ± 227	-
3	3.43	OPC-42.5N	22	9.05	no	2070.9 ± 8.0	-	3.28 ± 2.36	-	-
4	6.19	OPC-42.5N	22	9.05	no	2094.5 ± 2.9	-	11.68 ± 2.04	7081 ± 890	-
5	3.85	OPC-42.5N	12	9.05	no	2124.4 ± 17.1	-	2.72 ± 3.69	-	-
6	6.34	OPC-42.5N	12	9.05	no	2099.2 ± 2.6	7.40 ± 1.53	-	-	-
7	5.45	OPC-42.5N	12	9.05	yes	2045.2 ± 21.5	-	5.41 ± 0.65	4970 ± 384	-
8	9.33	OPC-42.5N	6	10.2	no	2254.0 ± 15.6	-	5.09 ± 0.73	6168 ± 751	-
9	3.43	CPC-42.5N	22	5.66	no	2002.0 ± 35.0	-	2.0 ± 1.23	-	-
10	5.64	CPC-42.5N	22	9.05	no	2070.7 ± 2.3	7.09 ± 1.95	-	-	-
11	3.85	CPC-42.5N	12	9.05	no	2083.9 ± 18.0	-	2.1 ± 1.51	-	-
12	7.96	OPC-42.5N	6	10.2	no	2243.1 ± 13.4	-	7.49 ± 1.24	7988 ± 409	-
13	5.2	OPC-42.5N	12	9.05	no	2112.6 ± 9.6	5.03 ± 0.56	7.53 ± 1.1	5049 ± 583	-
14	6.19	CPC-42.5N	22	9.05	no	2059.4 ± 6.8	-	9.98 ± 0.83	6689 ± 474	-
15	6.78	OPC-42.5N	22	9.05	no	2086.2 ± 31.4	-	10.42 ± 2.93	-	-
16	6.78	CEM III/B 32.5N-LH/SR	22	9.05	no	2090 ± 11.1	-	13.45 ± 1.89	6691 ± 1408	0.153 ± 0.032
17	7.95	OPC-42.5N	12	10.2	yes	2140.7 ± 11.0	-	15.49 ± 1.28	11161 ± 894	-
18	8.6	OPC-52.5R	12	9.05	yes	2199.5 ± 8.8	-	20.0 ± 1.65	13716 ± 866	0.113 ± 0.073
19	6.55	OPC-42.5N	12	10.2	no	2240.1 ± 12.9	8.92 ± 1.68	9.27 ± 2.52	6046 ± 762	-
20	7.95	OPC-42.5N	6	10.2	yes	2167.7 ± 12.5	-	10.73 ± 1.61	9714 ± 694	-
21	8.6	OPC-42.5R	12	9.05	yes	2168.5 ± 6.5	-	15.31 ± 1.29	11597± 1257	0.087 ± 0.049

22	6.55	OPC-52.5R	12	10.2	yes	2153.8 ± 15.0	-	14.4 ± 1.05	9955 ± 607	0.097 ± 0.046
23	7.95	OPC-52.5R	12	9.05	yes	2170.0 ± 8.1	-	17.06 ± 1.31	12615 ± 2059	0.156 ± 0.102
24	7.61	CPC-42.5N	6	9.05	no	2212.22 ± 9.96	-	6.94 ± 1.03	8324.3 ± 904.58	0.065 ± 0.0145
25	7.27	CPC-42.5N	22	9.05	no	2064.17 ± 23.38	-	10.75 ± 0.84	8469.2 ± 1057	0.17 ± 0.08
26	6.78	CPC-42.5N	12	9.05	no	2196.79 ± 8.38	-	11.69 ± 0.9	8460.17 ± 1839.66	0.03 ± 0.028
27	7.61	CPC-42.5N	12	9.05	no	2145.6 ± 7.1	-	11.65 ± 2.49	7650 ± 1363	0.133 ± 0.085
28	7.61	CPC-42.5N	12	5.66	no	2165.49 ± 16.84	-	8.89 ± 1.18	9103.76 ± 1796.18	0.09 ± 0.1041

%w: water content expressed as percentage by weight of dry mixture (coarse sand + excavated soil + cement)
b: type of binder like Ordinary Portland Cement "OPC" or Composite Portland Cement "CPC" of class 42.5N, 42.5R and 52.5R
%b: percentage of cement by weight of dry mixture
p: compaction pressure imposed by hydraulic press
GE: yes (grind earth), no (not grind earth)
BD: Bulk density after curing
C-7: 7-d compressive strength value
C-28: 28-d compressive value
EM: Elastic modulus
PR: Poisson's ratio

Finally, it is evident that with equal mixture composition a higher %b determines a higher strength value. In particular, it can be denoted that with the optimal %w (from 6.5 to 9%) high strength class of binder (from 42.5N to 52.5R) leads to higher mechanical performances on resulting PE mixtures (C-28 from 9 to 20 MPa). This result pointed out the analogy of strength development between PE and concrete, showing the interest to implement concrete model on SE. This aspect is currently investigated but is out of the topic of this paper. Output data values obtained by experimental testing on trial PE mixtures were processed in AMDCP which stopped the routing once it detected a trial PE mixture satisfying the control requirements (see Figure 4). In particular there are two series for which all of them are satisfied (series 27 and 28 labeled hereafter "PE-27" and "PE-28" respectively). As it can be observed in Table 4 and Figures 9 and 10, the mix-design used in PE-28 permitted to obtain closer values, than PE-27, to the mechanical performances of SE in regard to the threshold requirements defined at the control step of AMDCP. Consequently, input and output parameters of PE-28 were used to develop a constitutive relationship between mechanical performances of SE and PE. Formulations described in Eqns (2) permit therefore to predict the engineering properties of SE as engineering properties of PE are known, in particular BD, C-28, EM and PR.

$$BD_{SE} = 0.95BD_{PE}; \qquad C\text{-}28_{SE} = 1.07C\text{-}28_{PE};$$
$$EM_{SE} = 1.07EM_{PE}; \qquad PR_{SE} = 1.67PR_{PE}. \tag{2}$$

It is worth remembering that the mixture of PE-28 was composed by the same types and amounts of raw materials used to fabricate SE, in particular 7:7:2 of excavated soil:coarse sand:cement CPC-42.5N. The water content of PE-28 mixture was 7.61% (8.67% in SE) and the compaction pressure was 5.66 MPa. The latter proved to well simulate the compaction effect observed in SE during the projection at high speed, since BD_{SE} and $BD_{PE\text{-}23}$ are almost the same, see Equation 2. Table 4 summarizes the control criterion results obtained from the AMDCP.

Table 4. Control criterion results obtained from the *AMDCP*

Control requirements	$\varepsilon_{,w}$ %	$\varepsilon_{,b}$ -	$\varepsilon_{,\%b}$ -	$\varepsilon_{,BD}$ kg/m^3	$\varepsilon_{,C}$ MPa	$\varepsilon_{,EM}$ MPa	$\varepsilon_{,PR}$ -	Fitting quality
	2.2	0	1.2	206.7	2	971	0.03	
Series								
1	False	False	False	True	False	False	N.A.	14%
12	False	False	False	True	False	False	N.A.	14%
3	False	False	False	True	False	N.A.	N.A.	14%
4	False	False	False	True	True	False	N.A.	29%
5	False	False	True	True	False	N.A.	N.A.	29%
6	False	False	True	True	False	N.A.	N.A.	29%
7	False	False	True	True	False	False	N.A.	29%
8	True	False	False	True	False	False	N.A.	29%
9	False	True	False	True	False	N.A.	N.A.	29%
10	False	True	False	True	False	N.A.	N.A.	29%
11	False	True	True	True	False	N.A.	N.A.	43%
12	True	False	False	True	True	False	N.A.	43%
13	False	False	True	True	True	False	N.A.	43%
14	False	True	False	True	True	False	N.A.	43%
15	True	False	False	True	True	N.A.	N.A.	43%
16	True	False	False	True	False	False	True	43%
17	True	False	True	True	False	True	N.A.	57%
18	True	False	True	True	False	False	True	57%
19	True	False	True	True	True	False	N.A.	57%
20	True	False	False	True	True	True	N.A.	57%
21	True	False	True	True	False	True	True	71%
22	True	False	True	True	False	True	True	71%
23	True	False	True	True	False	True	True	71%
24	True	True	False	True	True	True	False	71%
25	True	True	False	True	True	True	True	86%
26	True	True	True	True	True	True	False	86%
27	True	True	True	True	True	True	True	100%
28	True	True	True	True	True	True	True	100%

$\varepsilon_{,w}$: maximum scatter between SE and PE in terms of water content, 10% of water content of SE, so 2.2%
$\varepsilon_{,b}$: logical transformation to compare the type of binder between SE and PE. "0" stands to "equal to SE binder"
$\varepsilon_{,\%b}$: maximum scatter between SE and PE in terms of percentage of cement, 10% of percentage of cement of SE, so 1.2%
$\varepsilon_{,BD}$: maximum scatter between SE and PE in terms of bulk density, 10% of bulk density of SE, so 206.7 kg/m^3
$\varepsilon_{,C\text{-}28}$: maximum scatter between SE and PE in terms of 28-d compressive, 20% of 28-d compressive strength of SE, so 2 MPa
EM: maximum scatter between SE and PE in terms of elastic modulus, 10% of Young modulus of SE, so 971 MPa
PR: maximum scatter between SE and PE in terms of Poisson's ratio, 20% of Poisson's ratio of SE, so 0.03

It should be mentioned that EM and PR tests were not performed for all PE series, but just for PE series where mechanical performances of PE were almost equal to those of SE.

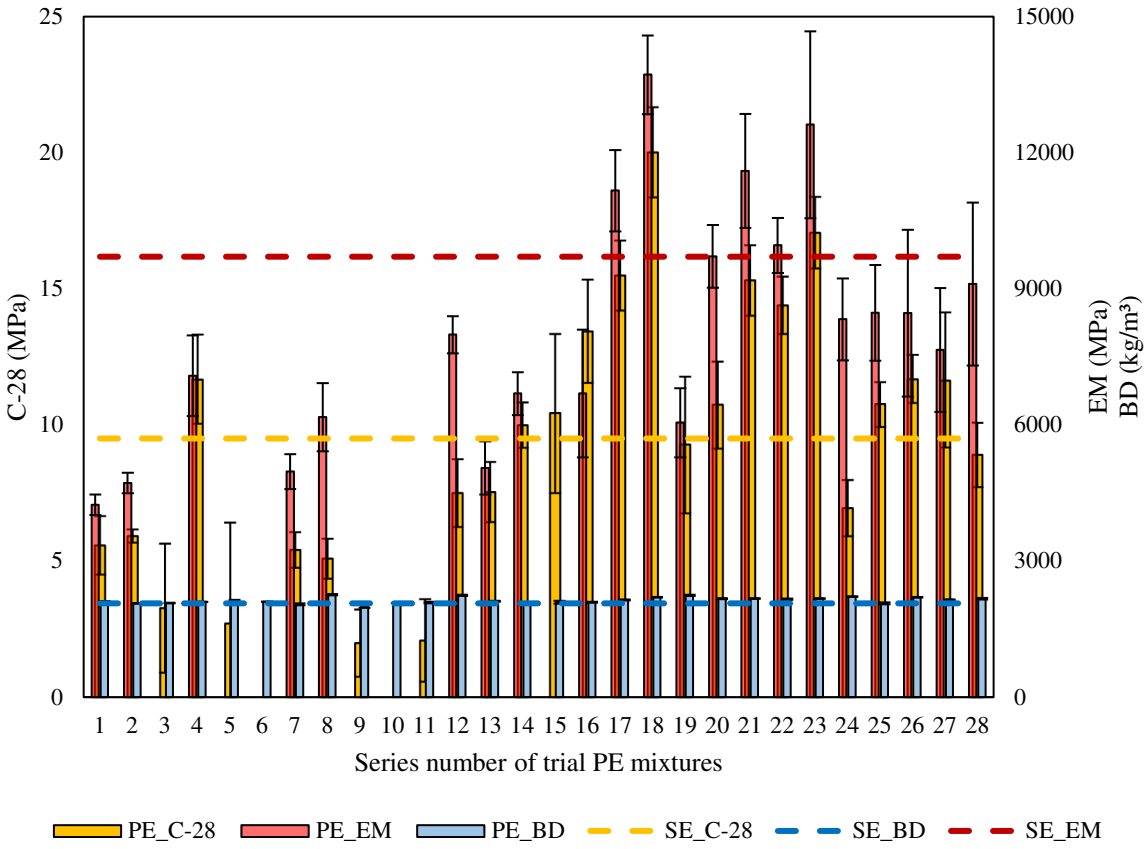

Figure 9. AMDCP results : output (BD, C-28, EM) and control (dotted lines) values at the end of process

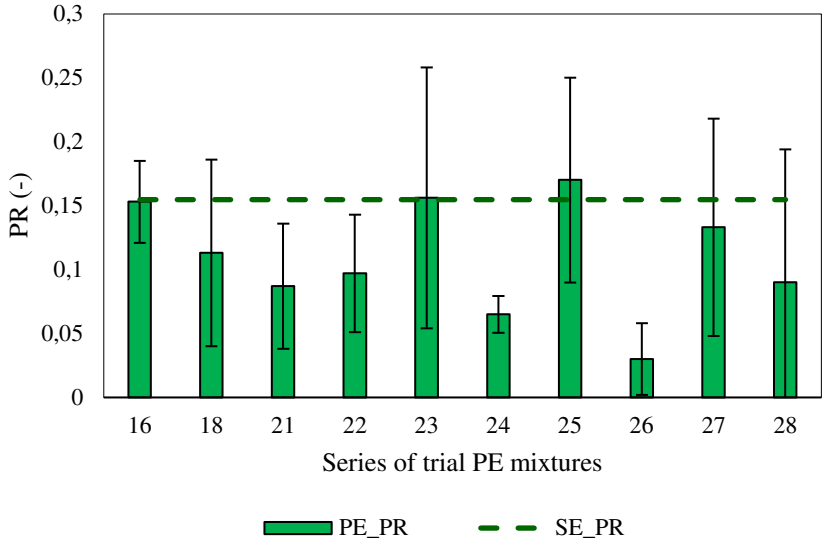

Figure 10. AMDCP results: output (PR) and control (dotted lines) values at the end of process.

4. Conclusions

For any earth-based composite construction material, a reliable mix-design strategy is essential. The mix-design strategy accounts for the variability of the waste/recycled material and allows predicting the

mechanical properties of the hardened material. Once the mechanical properties are available, the behavior of the material under load and its time-evolution can be predicted and provided to the structural engineers for safety and serviceability calculations. Shot-earth (SE), a new class of sustainable material made with high rates of excavation earth is no exception. Based on the test results of the presented research, it is possible to conclude that:

- A constitutive relationship between the mechanical performances of SE and those of pressed earth (PE) has been established.
- The developed constitutive relationship permits the determination of the mechanical characteristics of any SE mix using cost-effective and time-saving pressed earth specimens.
- An adaptive mix-design calibration process (AMDCP) has been developed to quickly identify the SE mix that will provide the hardened mechanical characteristics that best fit the structural engineer's requirements.

To sum up, SE proves to be an efficient construction material owing to the availability of mix-design strategies and design models. Additionally, the principles employed in its development can be readily applied to other composite earth-based materials.

Declaration of Competing Interest

The authors declare that they have no known competing financial interests or personal relationships that could have appeared to influence the work reported in this paper.

Acknowledgments

Financial support from the HES-SO in the framework of the projects « NextEarthBuild – Une nouvelle génération d'éco-construction en terre d'excavation recycle – n° 98528 » and « EcoAbri – Construction d'un abri témoin en terre d'excavation et autres matériaux écologiques et indigènes en vue de la réalisation ultérieure d'un espace de rangement non chauffé – n° 108222 » is gratefully acknowledged. Financial support from Innosuisse in the framework of the Project « Innosuisse – Shotearth : a sustainable excavated-soil based building material – n° 52127.1 IP-EE » is gratefully acknowledged as well. Financial support from the Italian Ministry of University and Research (MUR) in the framework of the Project FISR 2019: "Eco_Earth" (code 00245; CUP: B84G19000170008) is gratefully acknowledged. Finally, financial support from University of Modena and Reggio Emilia in the framework of "FAR Dipartimentale 2022-2023" (CUP: E93C22000590005) is gratefully acknowledged.

Data availability statement

The raw/processed data required to reproduce these findings cannot be shared at this time as the data also forms part of an ongoing study.

5. References

[1] M. Stevanovic, "Catalhöyük Excavations of a Neolithic Anatolian Höyük," 2005. [Online]. Available: https://www.catalhoyuk.com/archive_reports/2005/ar05_34.html. [Accessed 17 11 2022].

[2] A. Gattupalli, "Arch daily," 17 10 2022. [Online]. Available: https://www.archdaily.com/990660/the-science-behind-the-resilience-of-earth-architecture#:~:text=In%20the%20presence%20of%20atmospheric,sturdier%20in%20very%20dry%20conditions. [Accessed 17 11 2022].

[3] Britannica T. Editors of Encyclopaedia, "Great Wall of China. Encyclopedia Britannica.," 23 October 2022. [Online]. Available: https://www.britannica.com/topic/Great-Wall-of-China.

[4] Wikipedia, "Piramide del Sole di Teotihuacan," [Online]. Available: https://it.wikipedia.org/wiki/Piramide_del_Sole_di_Teotihuacan. [Accessed 20 12 2022].

[5] P. Jaquin, C. Augarde and C. Gerrard, "Chronological description of the spatial development of rammed earth techniques," *International Journal of Architectural Heritage,* vol. 2:4, pp. 377-400, 2008.

[6] L. Miccoli, U. Müller and P. Fontana, "Mechanical behaviour of earthen materials: A comparison between earth block masonry, rammed earth and cob," *Construction and building materials ,* vol. 61, pp. 327-339, 2014.

[7] L. Miccoli, R. Silva, A. Garofano and D. Oliveira, "In-plane behaviour of earthen meterials: a numerical comparison between adobe masonry, rammed earth and cob," *Conference: 6th International Conference on Computational Methods in Structural Dynamics and Earthquake Engineering (COMPDYN 2017),* vol. 1, pp. 2478-2504, 2017.

[8] H. Niroumand, M. Zain and M. Jamil, "Various Types of earth buildings," *Procedia - Social and Behavioral Sciences,* vol. 89, pp. 226-230, 2013.

[9] A. Curto, V. Savino and M. Viviani, "Modern Catalan vaults: FE analyses and experimental characterization," *Procedia Structural Integrity,* vol. 39, pp. 671-676, 2022.

[10] V. Savino, M. Franciosi and M. Viviani, "Engineering and analyses of a novel Catalan vault," *Engineering Failure Analysis,* vol. 143, 2023.

[11] J. P. Villacreses, J. Granados, B. Caicedo, P. Torres-Rodas and F. Yepez, "Seismic and hydromechanical performance of rammed earth walls under changing environmental conditions," *Construction and building materials,* vol. 300, 2021.

[12] S. Talibi, J. Page, C. Djelal, M. Waqif and L. Saâdi, "Study of earth-based materials for manufacturing compaction process," *Journal of Building Engineering,* vol. 64, 105546, 2023.

[13] M.-I. Lavie Arséne, C. Fredéric and F. Nathalie, "Improvement of lifetime of compressed earth blocks by adding limestone, sandstone and porphyry aggregates," *Journal of Building Engineering,* vol. 29, 101155, 2020.

[14] G. Lan, S. Chao, Y. Wang and K. Zhang, "Study of compressive strength test methods for earth block masonry—Capping method and loading mode," *Journal of Building Engineering,* vol. 43, 103094, 2021.

[15] The Tiny Life, "Cob Houses: A Simple Guide To Building A Cob House," [Online]. Available: https://thetinylife.com/cob-houses/. [Accessed 17 11 2022].

[16] R. Reitermann, "Archilovers," 5 10 2005. [Online]. Available: https://www.archilovers.com/projects/503/chapel-of-reconciliation.html. [Accessed 20 12 2022].

[17] B. Bühler, "ArchiTonic," [Online]. Available: https://www.architonic.com/en/project/boltshauser-architekten-rammed-earth-house-rauch-family-home/5100620. [Accessed 20 12 2022].

[18] L. M. Gil-Martín, M. A. Fernández-Ruiz and E. Hernández-Montes, "Mechanical characterization and elastic stiffness degradation of unstabilized rammed earth," *Journal of Building Engineering,* vol. 56, 104805, 2022.

[19] B. V. V. Reddy and R. S. Bhanupratap Rathod, "Influence of interlayer shear studs on the behaviour of cement stabilised rammed earth under compression, tension and shear," *Journal of Building Engineering,* vol. 49, 10409, 2022.

[20] T.-D. Nguyen, T.-T. Bui, A. Limam, T.-L. Bui and Q.-B. Bui, "Evaluation of seismic performance of rammed earth building and improvement solutions," *Journal of Building Engineering,* vol. 43, 103113, 2021.

[21] J. Morel, A. Mesbah, M. Oggero and P. Walker, "Building houses with local materials: means to drastically reduce the environmental impact of construction," *Building and environment ,* vol. 36, pp. 1119-1126, 2001.

[22] E. Araldi, E. Vincens, A. Fabbri and J.-P. Plassiard, "Identification of the mechanical behaviour of rammed earth including water content influence," *Mater struct,* vol. 51, 2018.

[23] M. S. Zami, "Counterbalancing benefits and drawbacks of contemporary stablised earth construction by construction professionals," *Archnet-IJAR,* vol. 5, pp. 49-62, 2011.

[24] A. W. Bruno, D. Gallipoli, C. Perlot and J. Mendes, "Mechanical behaviour of hypercompacted earth for building construction," *Mater Struct,* vol. 50, 2017.

[25] A. Curto, L. Lanzoni, A. M. Trantino and M. Viviani, "Shot-earth for sustainable constructions," *Construction and building materilas,* vol. 239, 2020.

[26] M. Bacciocchi, V. Savino, L. Lanzoni, A. M. Tarantino and M. Viviani, "Multi-phase homogenization procedure for estimating the mechanical properties of shot-earth materials," *Composite Structures,* vol. 295, 2022.

[27] S. Vantadori, A. Zak, Ł. Sadowsky, C. Ronchei, D. Scorza, A. Zanichelli and M. Viviani, "Microstructural, chemical and physical characterisation of the Shot-Earth 772," *Construction and building materials,* vol. 341 (127766), 2022.

[28] A. D'Alessandro, C. Fabiani, A. Pisello, F. Ubertini, A. Materazzi and F. Cotana, "Innovative concretes for low-carbon constructions: a review," *International Journal of Low-Carbon Technologies,* vol. 12(3), pp. 289-309, 2017.

[29] A. D'Alessandro, A. Meoni and F. Ubertini, "Stainless Steel Microfibers for Strain-Sensing Smart Clay Bricks," *Journal of Sensors,* 2018.

[30] L. Boquera, E. Olacia, C. Fabiani, A. Pisello, A. D'Alessandro, F. Ubertini and L. Cabeza, "Thermo-acoustic and mechanical characterization of novel bio-based plasters: The valorisation of lignin as by-product from biomass extraction for green building applications," *Construction and Building Materials,* vol. 278, 2021.

[31] A. D'Alessandro, A. Meoni, V. Savino, M. Viviani and F. Ubertini, "New self-sensing shot-earth cement-composites for smart and sustainable constructions: experimental validation on a full-scale vault," *Proceedings of 6th Workshop on The New Boundaries of Structural Concrete 2022 University of Salento – ACI Italy Chapter Lecce, Italy, September 8-9,* pp. 151-160, 2022.

[32] B. Venkatarama Reddy and P. Prasanna Kumar, "Cement stabilised rammed earth. Part A: compaction characteristics and physical properties of compacted cement stabilised soils," *Material and structures,* vol. 44, pp. 681-693, 2011.

[33] B. Venkatarama Reddy and P. Prasanna Kumar, "Cement stabilised rammed earth. Part B: compressive strength and stress–strain characteristics," *Materials and structures ,* vol. 44, pp. 695-707, 2011.

[34] J. Canivell, J. J. Martin-del-Rio, F. Alejandre, J. García-Heras and A. Jimenez-Aguilar, "Considerations on the physical and mechanical properties of lime-stabilized rammed earth walls and their evaluation by ultrasonic pulse velocity testing," *Construction and building materials ,* vol. 191, pp. 826-8336, 2018.

[35] "SN 670 340-1 Reconnaissance et essais géotechniques – Essais de laboratoire sur les sols – Partie 1: Détermination de la teneur en eau".

[36] SADCSTAN, Rammed earth structures - Code of practice THC 03, African Organisation for Standardisation, 2014.

[37] "UNI EN 12390-3:2003 - Testing hardened concrete - Compressive strength of test specimens".

[38] "EN 13412:2006 - Products and systems for the protection and repair of concrete structures - Test methods - Determination of modulus of elasticity in compression".

[39] C469/C469M-14, Standard test method for static modulus of elasticity and Poisson's ratio of concrete in compression, ASTM, 2014.